IEEE Access
Multidisciplinary | Rapid Review | Open Access Journal

Date of publication xxxx 00, 0000, date of current version xxxx 00, 0000.

Digital Object Identifier 10.1109/ACCESS.2019.DOI

Optimal Mode Selection for Full-Duplex Enabled D2D Cognitive Networks

NOMAN HAIDER[1], AHSAN ALI[2], CRISTO SUAREZ-RODRIGUEZ[1], (Member, IEEE), ERYK DUTKIEWICZ[1], (Senior Member, IEEE)

[1]University of Technology Sydney, Global Big Data Technology Centre, Ultimo NSW 2007, Australia.
[2]Department of Engineering, Macquarie University, Australia.

Corresponding author: Noman Haider (e-mail: noman90@ieee.org).

ABSTRACT Full-Duplex (FD) and Device-to-Device (D2D) communications have been recognized as one of the successful solutions of spectrum scarcity in 5G networks. Significant advancements in self-interference-to-power-ratio (SIPR) reduction have paved the way for FD use to double the data rates and reduce the latency. This advantage can now be exploited to optimize dynamic spectrum sharing among different radio access technologies in cognitive networks. However, protecting the primary user communication has been a challenging problem in such coexistence. In this article, we provide an abstract level analysis of protecting primary users reception based on secondary users FD enabled communication. We also propose optimal mode selection (Half-duplex, Full-duplex, or silent) for secondary D2D users depending on its impact on primary users. Our analysis presents the significant advantage of D2D mode selection in terms of efficient spectrum utilization while protecting the primary user transmission, thus, leading the way for FD enabled D2D setup. Depending on the location and transmit power of D2D users, the induced aggregate interference should not violate the interference threshold of primary users. For this, we characterize the interference from D2D links and derive the probability for successful D2D users for half-duplex and full-duplex modes. The analyses are further supported by theoretical and extensive simulation results.

INDEX TERMS 5G, Cognitive Networks, Stochastic geometry, Full Duplex, Device-to-Device, interference protection, success probability, guard zone.

I. INTRODUCTION

THE gigantic increase in a number of connected users and devices to the internet complemented by significant growth in mobile applications has aggressively challenged the capacity of existing communication systems and demanded multi-gigabits per second data rates. To cope with such increase, advancements in all aspects from access to the core network are required along with the performance elevation of key network resources. The capacity of existing and future telecommunication systems highly relies on effective spectrum utilization. Because, spectrum is a key resource or carrier which connects users to the internet. In recent years, optimization of spectrum usage among sharing stakeholders played a vital role in the evolution of Next Generation Networks (5G). Along with the addition of new spectrum space for mobile systems in 5G [1], innovative proposals have been made to employ different spectrum sharing options to further elevate the system capacity [2].

Spectrum sharing frameworks have significantly proven their performance advantages and played a vital role in optimizing the user capacity and socio-economic benefits of existing communication systems [3]. Among these proposals, Cognitive Radio (CR), TV white spaces, Citizen Broadband Radio Service (CBRS) and Licensed Shared Access (LSA) have proven to be an effective solution for spectrum underutilization. The key aim is to increase spectral efficiency on the basis of use-it or share-it basis, where, Primary Users (PUs) can share/lease underutilized spectrum on a short-to-short or short-to-long term basis with Secondary Users (SUs). This sharing is done based on pre-defined conditions for leaving the spectrum for priority users whenever needed and imposing the least interference to PUs. The Spectrum sharing can be done in the time domain (primary user is not transmitting), space domain (primary user is far away) and frequency domain (primary user is transmitting on a different frequency). For detailed benefits of dynamic spectrum

This article has been accepted for publication in a future issue of this journal, but has not been fully edited. Content may change prior to final publication. Citation information: DOI 10.1109/ACCESS.2019.2913538, IEEE Access

sharing and heterogeneous device coexistence, readers are referred to [4].

The key enabling technology candidates in 5G further paved the way for higher gains in improving spectrum efficiency using Dynamic Spectrum Sharing (DSA) [5]. Among these technologies, Device-to-Device (D2D), massive MIMO, Full-Duplex (FD) radios, millimeter wave and Terahertz band, multi-Radio Access Technologies (multi-RATs) and Network Virtualization are spotlight candidates. The performance gains offered by these enabling technologies can be multifold after thorough feasibility studies for their practicality to be integrated into cellular systems [6]. Such technologies have complemented and elevated significantly machine-type communications in pursuit of accelerate automation and industrial revolution [7].

The rest of the paper is organized as follows. The related work, motivation, and contributions are presented in section II. The detailed system model, the problem addressed propagation assumptions and received power expressions are provided in section III. Then, we investigate the D2D mode selection (HD/FD/Silent) based on interference conditions in section IV. The probability of success for primary and secondary users and respective interference fields are characterized and analyzed in section V. Simulation, preliminary theoretical results and discussion are presented in section VI. Finally, the conclusion of the paper and future research directions are given in section VII.

II. RELATED WORK AND MOTIVATION

The recent significant advancements in self-interference-to-power-ratio (SIPR) reduction have paved the way for use of full-duplex radios to double the data rates at the cost of induced interference. For instance, practically the cancellation capability of 70dB can be achieved using compact/separated antennas at the bandwidth of 100MHz in 2.6GHz band [8]. Thus, in-band FD communications integrated with D2D technology will elevate the spectral efficiency while doubling the data rates [9]. Moreover, recent research has also indicated toward the elevation of spectral efficiency (up to 100%) in single-cell and single D2D link scenarios as compared to half-duplex (HD) if sufficient SIPR is achieved [10]–[12]. However, without considering the impact of induced interference from FD mode, it may cause more harm than benefit. Thus, an interesting research problem needs further work to find a feasible trade-off between the use of FD radio while limiting the induced interference, which is also the motivation behind this work. In this article, we study the use of FD equipped D2D devices as secondary users and propose mode switching between half-duplex and full-duplex based on interference faced by primary users. The recently published and closely related work in [13] presented detailed insight into Spatial Spectrum Sensing based D2D enabled cellular networks, where HD D2D network is modelled as Poisson Hole Process (PHP) and relevant interference characterizations along with upper and lower bounds were well studied, however, we consider FD enabled D2D setup in this work. Another work in [14] presents stochastic geometry based comprehensive and detailed analysis on Full-Duplex communications for cache-enabled D2D networks. Different operating modes, their probabilities and content-based caching have been discussed.

We use Stochastic Geometry (SG) analysis which is proven to be an effective mathematical platform in previous works to model variants of communication networks while characterizing the key network parameters [15]. For instance, the authors in [16] present stochastic geometry analysis of coverage and performance of D2D network from a user association model based on multiple simultaneous requests in homogeneous systems and ultra-dense small networks. Due to topological and spatial randomness, SG can successfully yield tractable, and in special cases, closed-form expressions that reflect the system behavior. The alternate methods for performance evaluation of cellular networks include exhaustive simulation scenarios to average out the randomness of different network parameters (base stations, user locations and fading distributions). However, these methods are time-consuming and prone to errors. Therefore, SG provides a supplementary platform to produce baseline results for benchmarking, and comparative performance analysis [17].

The comprehensive tutorial on SG modeling, design, and analysis for multi-tier and cognitive cellular networks is presented in [18]. Interference characterization and relevant analytical tools are comprehensively discussed. Another related work in [19] characterized D2D throughput based on social interaction and distance distribution in the context of spectral efficiency. Moreover, link-distance based mode selection along with link-distance distribution in different social scenarios was proposed to decrease the communication probability density.

Authors in [20] proposed SG-based modeling of carrier sensing based multiple access schemes for cognitive radio networks. Protection zones were considered among PUs where SUs will not be retained and are not allowed to transmit. The baseline work for coverage and rate analysis

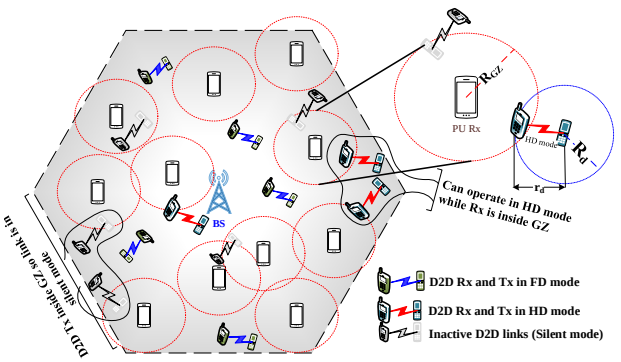

FIGURE 1: Realization of considered network model in single cell scenario with cellular guard zones and D2D Links (silent, HD and FD mode).

in cellular networks was published in [21], which also highlighted tractability of SG tools and comparative performance analysis with a SG model, a grid model, and actual network deployment. Another work [22] studied the stochastic geometry of thinned nodes to capture the knowledge of the post-MAC geometrical distribution of nodes as thinning mechanisms alter the spatial distribution. Circular Guard Zones (GZs) were drawn around the intended receiver to protect its reception by inhibiting close-by transmissions. A similar concept is adopted in this article to protect PUs reception and investigated if SU should switch to HD, FD or silent mode. Moreover, the SG analysis for interference characterization and expressions for network performance metrics for K-tier heterogeneous cellular networks is presented in [23]. One of the closely related work [24] modeled PUs and cognitive users (CUs) as an independent Poisson, Point Processes (PPPs). An exclusions zones (where cognitive cannot transmit) were drawn around PU such that CUs form PHP. Due to inter-dependence between PUs and CUs along with overlap of protection zones (PZs), the interference upper and lower bounds were given along with the practicality of implementing Poisson cluster process on such networks. Most of these works have employed SG analysis and modeling of PUs and SUs with HD only, however, in this article, we assess the impact of FD D2D enabled SUs while guarding PUs reception in up-link and characterize the interference for mode selection (HD, FD or silent). The network realization in a single-cell scenario considered in this article is presented in Fig. 1.

In the context of dynamic spectrum sharing, recently SG modeling and analysis of CBRS is done in [25]. Authors present a tractable performance analysis of CBRS by employing PZs for priority access licensed (PAL) users, while general authorized access (GAA) users operate using the contention-based channel access mechanism (CSMA). A similar approach of employing guard zones (GZ) has been used in [26], SG analysis for co-existence of contention-based (WiFi) and scheduled based (LTE) networks is presented in [27]. SG analysis of FD D2D has also been recently studied and performance trade-offs have been assessed in [14]. The initial SG analysis for throughput of wireless networks equipped with FD capability and imperfect SIPR was done in [28]. Another SG approach presented signal to interference and noise ratio (SINR), transmit-power and mode switching (HD/FD) for FD D2D for cellular networks [9]. Authors in [14] presented performance analysis of FD in cache-enabled D2D networks but the emphasis is kept more on the content caching, sharing and delivery, whereas, our work focuses more on cognitive type setup with FD D2D users.

The key motivation of this work is driven by the fact that critical mode selection analysis of adjacent secondary users while protecting primary user receptions would elevate the spectral efficiency alongside making more space and opportunities for ultra-dense networks in future urban scenarios. As this work focuses especially on the secondary users lying in the vicinity of the edge of PUs GZ, the analysis will study the limits to which secondary user can still communicate while near to the boundary of PUs GZ. Such opportunistic lending of spectral resources benefits both network operators (licensed operators), and license-free service providers. To the best of our knowledge, none of the existing works proposes the mode selection for FD enabled secondary users to protect the primary users receptions in the context of SG.

A. CONTRIBUTIONS

In this work, a SG framework for an optimal mode selection for D2D users enabled with half-duplex and full-duplex capabilities is proposed, while, protecting receptions of primary users. Specifically, each primary user reception is protected and D2D users opt for a mode based on their proximity to primary users. The main contributions of this work are summarized as follows:

- The induced interference from FD use of D2D devices and overall aggregate interference is characterized using SG tools. The trade-off between interference introduced by FD operation and spectral efficiency due to FD is critically investigated.
- We propose a novel mechanism for mode selection by D2D devices depending on receivers vicinity to PUs guard zones while assuring it doesn't impact the PUs reception for dynamic spectrum sharing frameworks. The proposed mode selection mechanism encourages primary licensees to allow SU operation either in HD or FD modes as long as SUs provide agreed upon interference protection to PUs.
- The paper presents quantified performance gains for opportunistic spectrum use complemented by FD radios in terms of probability of successful receptions by both cellular and D2D users. Using the expressions for coverage probabilities, we also present insights into different GZ radius values and their impact on SUs communication.

III. SYSTEM MODEL

We consider a heterogeneous wireless network, where the primary user (cellular operator) allows secondary users (D2D) to opportunistically use the spectrum conditioned on interference protection for cellular users. The leased spectrum is segregated into small chunks, we assume PU is operating on one of these selected frequency bands for downlink reception. The second-tier users can be inferred as ultra-dense small networks dynamically sharing spectrum with tier-1 users. Specifically, we focus on D2D users as secondary users (SU), enabled with Full-Duplex (FD) transceivers, which opportunistically use cellular spectrum conditioned on preset Interference Protection. The analysis is equally applicable on similar technologies which can operate as SUs with FD capabilities. The D2D users can opportunistically share incumbents spectrum outside of the GZs. Moreover, these FD enabled D2D transceivers can switch between the modes depending upon the induced interference to PUs.

This article has been accepted for publication in a future issue of this journal, but has not been fully edited. Content may change prior to final publication. Citation information: DOI 10.1109/ACCESS.2019.2913538, IEEE Access

The self-interference leakage in FD links is considered to be imperfect with a residual self-interference-to-power-ratio factor β. The value of β ranges from 0 to 1, from perfect to imperfect SIPR cancellation, respectively. The link-state of the D2D communication pair is half-duplex, full-duplex or silent.

A. SPATIAL LOCATIONS AND DISTANCE DISTRIBUTION

We consider a two-tier wireless network, in which the full-duplex enabled D2D users can opportunistically share the spectrum with tier-1 cellular users, also referred to as primary users (PUs). The locations of all the cellular users are modeled via an independent homogeneous PPP Φ_c with an intensity of λ_c in a single cell, while, the D2D transmitters are modeled via another homogeneous PPP which we denote as Φ_d, with intensity of λ_d. The PU's communication (reception in our model) must be protected from any harmful interference of SUs as required in most of Dynamic Spectrum Sharing (DSS) systems. In order to protect the reception of PU, we employ circular GZs of radius R_{GZ} centered at the locations of cellular users i.e. $x \in \Phi_c$. We denote this circular GZ around a cellular user located at x with radius R_{GZ} by $C_{x,R_{GZ}}$. The total area covered by all these circles with radius R_{GZ} can be expressed as [29],

$$\mathcal{A}_T \triangleq \bigcup_{x \in \Phi_c} C_{x,R_{GZ}}. \tag{1}$$

To protect the reception of cellular users from harmful interference of D2D transmitters, we delete the D2D Txs (points) from a ground PPP i.e. $y \in \Phi_d$ which lie inside the GZs of the primary users. Hence, the resulting point process of retained points will be Poisson-Hole Process (PHP) denoted by φ_d,

$$\varphi_d = \{y \in \Phi_d : y \notin C_{x,R_{GZ}} s.t. x \in \Phi_c\}, \tag{2}$$

which states that for a point $y \in \Phi_d$ to be retained in $y \in \varphi_d$, y should not be inside any of the circular GZ around primary receivers ($C_{x,R_{GZ}}$). The resulting intensity of φ_d is the number of points outside the GZs given by $\tilde{\lambda}_d$ [25],

$$\tilde{\lambda}_d = \lambda_d \exp(-\pi \lambda_c R_{GZ}^2), \tag{3}$$

Now, the D2D transmitters outside GZs (in Eq. 2) can transmit and form a communication link with receivers. To model the location of the D2D receivers for these transmitters $y \in \varphi_d$, we assign a mark m_y which is uniformly and randomly distributed on a circle of radius r_d centered at D2D Tx. The D2D communication link formed between transmitter y and receiver m_y has distance of r_d. The mark m_y can also be represented as, $m_y = y + r_d(\cos(\theta), \sin(\theta))$, where the angle θ is independently and uniformly distributed on $[0, 2\pi)$. These marks (m_y) form another point-process which we denote by φ_{m_d}. It should be noted here that m_y may lie inside the GZ of the cellular user, but it will not impact the reception of PU as the Tx (y) of D2D is still outside. However, its probability to go into half-duplex or full-duplex mode may change depending upon its location and angle θ. We will discuss this in detail in Section IV. The realization of the considered system model is presented in Fig. 1.

TABLE 1: Notations, Symbols and Description

Notation	Description
Φ_c, λ_c	PPP for cellular users, and its intensity
Φ_d, λ_d	PPP modeling of D2D transmitters, and its intensity
$\varphi_d, \tilde{\lambda}_d$	PHP of D2D transmitters from ground PPP of Φ_d, and its intensity
$\varphi_{m_d}, \tilde{\lambda}_{m_d}$	Marks (RXs) of D2D transmitters, and their intensity
$C_{x,R_{GZ}}$	Circular guard zone centered at $x \in \Phi_c$ with radius R_{GZ}
θ	The angle between D2D transmitter y and receiver m_y
$b(o,R)$	Circular disc of Radius R centered at origin $(0,0)$
$\mathcal{C}_1$	Annulus area of interest in ring formed by region $b(o,R_{GZ}) \cap b(o,R_{GZ}+R_d)$
$F_{o,\kappa}$	Channel fading at origin from user $\kappa = x, y, m_y$
α_c, α_d	Path-loss component for primary and D2D users
β	Residual self-interference-to-power ratio (SIPR) for FD nodes
T	SIR threshold for successful communication
R_{GZ}	Radius of guard zone around primary users
r_d, R_d	Random and fixed distance for D2D communication link
R_c	Fixed distance between typical cellular user and tagged base station

B. PROPAGATION MODEL

Random wireless channel effects are taken into account for performance analysis. We assume that each link in a considered wireless network described above experiences an i.i.d Rayleigh fading denoted by $F_{o,\kappa} = \exp(1)$ i.e. fading at typical receiver located at origin (o,o) from any point κ, which can can take values from, $x \in \Phi_c, y \in \varphi_d, m_y \in \varphi_{m_d}$. Also, we use notation $l(d)$ generically for path-loss of a communication link with distance d. For large scale fading we assume a distance based path loss model i.e. $d^{-\alpha_c}$ ($d^{-\alpha_d}$) for cellular and D2D links. Similarly, the transmit power will be P_c (P_d). For the typical cellular receiver the received power from the tagged base station (x_{BS}) located at a fixed distance of R_c can be written as:

$$P_r(x_o, x_{BS}) = P_c F_{x_o,x_{BS}} l(x_o, x_{BS}), \tag{4}$$

while, $l(x_o, x_{BS}) = R_c^{-\alpha_c}$. Similarly, we can write the intended received signal power at a D2D probe receiver as,

$$P_r(m_o, y_o) = P_d F_{m_o,y_o} l(m_o, y_o), \tag{5}$$

where, $l(m_o, y_o)$ represents the distance based path loss which is given by $l(m_o, y_o) = ||m_o - y_o||^{-\alpha_d}$, while, $||.||$ is Euclidean norm operator and F_{m_o,y_o} is the respective channel gain.

C. PERFORMANCE METRICS

The typical receiver (at the origin) can successfully receive from a tagged (intended) transmitter if SIR requirement is met at the receiver. The SIR success probability of a typical

This article has been accepted for publication in a future issue of this journal, but has not been fully edited. Content may change prior to final publication. Citation information: DOI 10.1109/ACCESS.2019.2913538, IEEE Access

receiver is the probability of achieving the target SIR threshold T,

$$p_s(T) \triangleq \mathbb{P}(\text{SIR}_{\mathcal{X}} > T), \tag{6}$$

where, $\mathcal{X}$ represents the probe receiver under consideration for analysis which is either cellular (x_o) or D2D user (m_o). Now, the SIR at a typical receiver is the ratio of the intended received signal power to total interference power from the rest of users. For ease of notational understanding, the interference term ($\mathcal{I}_{m_o,y\setminus y_o}$) means the interference received from all active D2D transmitters ($y \in \varphi_d$) except from intended transmitter i.e. y_o. For instance, the SIR of probe receivers in case of cellular and D2D links are given as follows,

$$SIR^c_{x_o} = \frac{P_c F^c_{x_o,x_{BS}} l\left(x_o, x_{BS}\right)}{\mathcal{I}_{x_o,y} + \mathcal{I}_{x_o,m_y}\mathbb{1}^{FD}_{m_y,y}}, \tag{7}$$

$$SIR^d_{m_o} = \frac{P_d F^d_{m_o,y_o} l\left(m_o, y_o\right)}{\mathcal{I}_{m_o,x} + \mathcal{I}_{m_o,y\setminus y_o} + \mathcal{I}_{m_o,m_y}\mathbb{1}^{FD}_{m_y,y} + \beta P_d \mathbb{1}^{FD}_{m_y,y}}. \tag{8}$$

The last term in Eq. 8 is due to SIPR from the antenna of the typical receiver if it is operating in the full-duplex mode and will be 0 in case the typical link is in the half-duplex mode. Without loss of generality, we can assume that our probe receiver is located at the origin which is permissible due to Slivnyak's theorem for PPP [30]. The conclusions drawn from the analysis of the system model described above is equally applicable to all the other users in the network due to the stationarity of PPP. Symbols, definitions and corresponding simulation values are listed in Table 1.

IV. MODE SELECTION

In this section, we derive the probability of the communication mode for a D2D link to be in silent, half-duplex or full-duplex mode based on its transmitter's distance to nearby cellular user GZ. The main objective is to protect cellular user reception from harmful interference of the D2D link. As the interference is mainly dependent on the distance of nearby interferes, the reception mode of the D2D receiver primarily depends on its distance from the primary user, the angle θ on a disk of radius r_d and how much inside it is in the guard zone.

D2D Link Distance Distribution: In the context of a D2D communication link distance distribution (r_d), it depends on the underlying application and social interactions among the users. For instance, in the case of the congested audience in the stadium would result in smaller r_d, and would be higher in a typical urban scenario. One of the trivial distance distributions for D2D users is formulated in [31], based on power-law communication probability ($0 \leq \vartheta < 2$) the PDF of D2D communication distance r_d is given by,

$$f_{r_d}(v) = \frac{(2-\vartheta)v^{1-\vartheta}}{R^{2-\vartheta}_{dmax}}, \tag{9}$$

where, v is a Random Variable (RV) representing D2D link distance r_d, R_{dmax} is the maximum communication

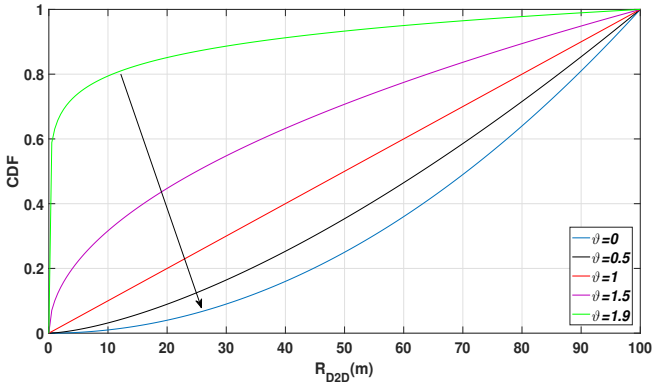

FIGURE 2: CDF of D2D Link Distance for different values of ϑ (social interaction parameter) as a function of D2D link-distance

distance of the D2D link and ϑ is the control parameter for the contact distance distribution (depends on social interaction of D2D users). Setting the value of $\vartheta = 0$ will make $f_{r_d}(v)$ independent of social-interaction and will result in a uniform distribution of D2D Rx in a circle of radius R_{dmax}, centered at D2D Tx as in [32].The CDFs for different D2D link distances and θ values are shown in Fig. 2. As, we start increasing the value of ϑ, the CDF of the D2D link distance approaches to 1 as ϑ reaches to 2. Thus, ϑ can be set according to social-interaction scenarios depending upon the density of D2D users ($\tilde{\lambda}_d$). The receivers (m_y) is uniformly distributed inside a disc of radius r_d taking values from pdf (f_{r_d}), where maximum possible distance can be R_{dmax}. In this work, we have considered fixed D2D link distance, R_d to reduce the mathematical complexity and closed-form expressions for the key performance metrics.

Let's consider cellular user x_o located at origin (o, o) also referred to as a typical cellular user, connected to base station x_{BS} at distance R_c. Now, we are interested to analyze the impact of the distance of x_o to nearby D2D transmitter y, referred to as $r_{x_o,y}$. From Fig. 3, depending on the distance ($r_{x_o,y}$) between the location of the primary user (i.e. center of its GZ) and the D2D transmitter (with Rx on a disk of radius R_d and angle θ), the communication modes for the D2D link can then be chosen safely to protect x_o reception. All the possible case scenarios which may emerge based on distance ($r_{x_o,y}$) are illustrated in Fig. 3 and discussed in detail in the following subsections.

A. CASE 1: D2D USERS IN SILENT MODE

In this case, the D2D communication pair is inside GZ of cellular receiver (x_o), then as per the interference protection conditions, x_o's reception must be protected and the D2D pair will not be active (remain in silent mode). This case was also used for D2D transmitters thinning in the system model in Eq. 2 where users inside the GZs were deleted. Alternatively, the D2D link will remain silent if the following

This article has been accepted for publication in a future issue of this journal, but has not been fully edited. Content may change prior to final publication. Citation information: DOI 10.1109/ACCESS.2019.2913538, IEEE Access

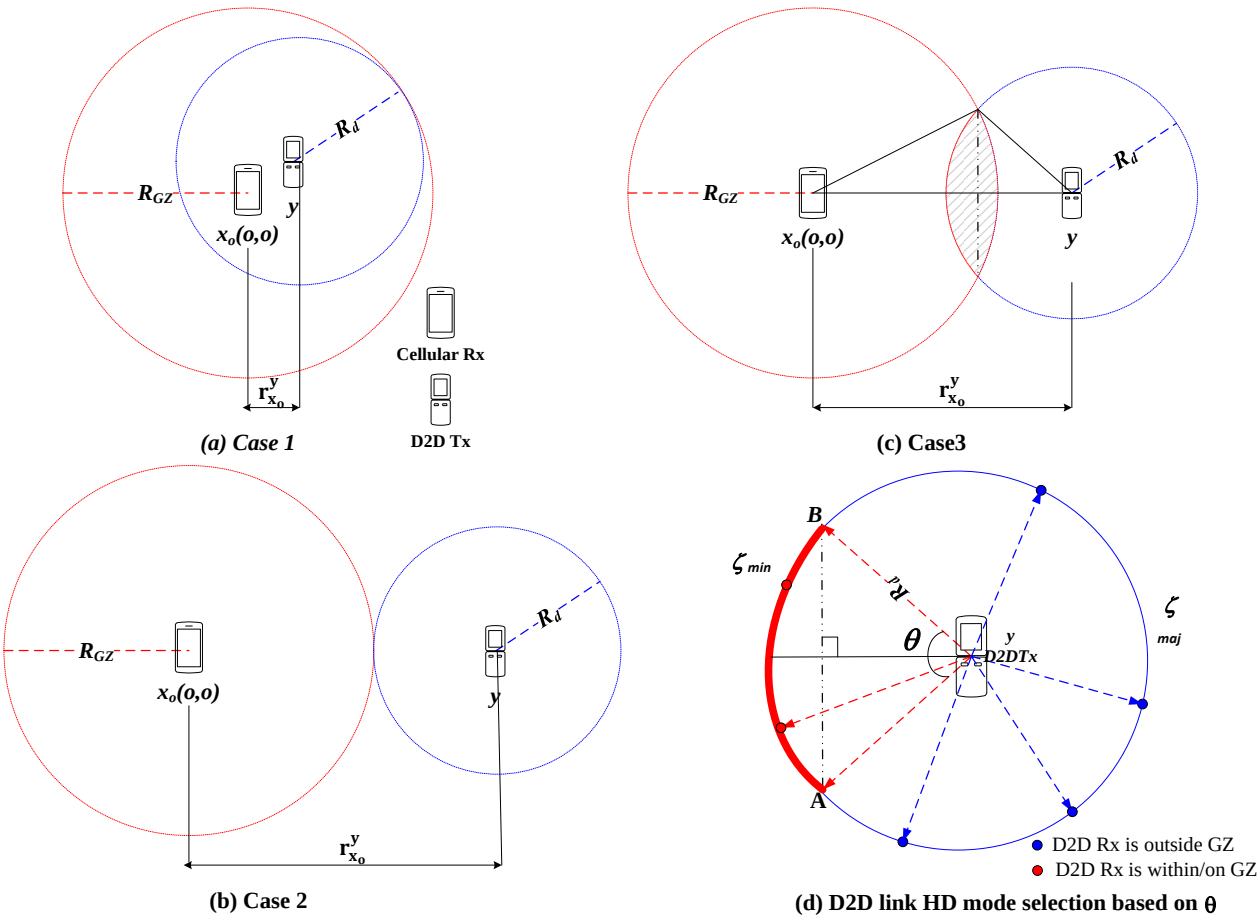

FIGURE 3: Illustration of possible case scenarios for D2D communication pair based on the distance between D2D transmitter and guard zone of cellular receiver

distance-based condition is met,

$$r_{x_o,y} < R_{GZ} \tag{10}$$

This scenario is also shown in Fig. 3 (a). We can represent the counting measure of D2D Txs in silent mode using random set formalism, where $\Phi_d \subset \mathbb{R}^2$ over an area of interest $|A|$ is a countable random set of D2D transmitters,

$$\Lambda_{sil} = \sum_{y_i \in \Phi_d, 0<||Y_i||\leq R_{GZ}} \mathbb{1}(y_i \in |A|) = \pi\lambda_d R_{GZ}^2 \tag{11}$$

Lemma 1: Considering disk $b(o, R_{GZ})$ of radius R_{GZ} at origin o, the probability of any D2D communication link to be in silent mode can be expressed as,

$$p_{sil} = \frac{\pi\lambda_d (R_{GZ})^2}{|A|} \tag{12}$$

Proof: Proof is given in Appendix VIII-A. Fig. 7a presents the analytical and simulation results of p_{sil}. The number of D2D users to be inactive directly depends on the radius of the guard zone, which ensures strong protection for cellular receiver, however, decreases the intensity of active D2D links.

B. CASE 2: D2D RECEIVERS IN HALF-DUPLEX MODE

The critical scenario is where a D2D receiver is either on the boundary of GZ or inside GZ (shaded area in the overlap region in Fig. 3 (b) and a D2D transmitter is outside GZ. The D2D link will be in the HD mode if m_y is inside GZ or on the guard zone to ensure protection for cellular receivers and will be in the FD mode if m_y is outside GZ (IV-C). Such a scenario can analytically be expressed as,

$$R_{GZ} < r_{x_o,y} < R_{GZ} + R_d. \tag{13}$$

while, m_y is insize GZ.

Now, we will evaluate the probability of the D2D link to communicate in the half-duplex mode. The important region which impacts the cellular user's reception greatly is the ring-shaped overlap region between circle $b(o, R_{GZ})$ and $b(o, R_{GZ} + R_d)$, denoted by $\mathcal{C}_1$ and shown as the highlighted region in Fig. 4. In region $\mathcal{C}_1$, the D2D links are segregated based on the angle (θ) and location of receiver m_y on circle $b(y, R_d)$ of radius R_d. Based on the angle $\theta(y, m_y)$, the probability of the D2D link to be either in the half-duplex or full-duplex mode can be derived.

Lemma 2: Given cellular user located at the origin with guard-zone $b(o, R_{GZ})$ and a D2D transmitter inside region $\mathcal{C}_1$, the D2D link will be in the half-duplex mode if receiver m_y exists on the minor arc (ζ_{min}) of the overlapping area between $b(o, R_{GZ}) \cap b(y, R_d)$,

$$\zeta_{min} = 2 \arcsin \left(\frac{\sqrt{4r_{x_o,y}^2 R_{GZ}^2 - \left(r_{x_o,y}^2 - R_d^2 + R_{GZ}^2\right)^2}}{2R_d r_{x_o,y}} \right). \tag{14}$$

Proof: Proof is given in Appendix VIII-B.

Thus, each D2D communication link can operate in the half-duplex mode if its receiver is located on the minor arc ζ_{min} as shown in Fig. 3 (d). Equipped with the expression for ζ_{min}, we can now proceed to find the intensity and probability of D2D transmitters which can operate in the HD mode. Based on this probability, the D2D communication pair can still operate in the HD mode as this will not violate the interference protection (IP) given to the primary user, but increases spectral efficiency and capacity for D2D users (SUs). The counting measure of D2D users that will operate in HD mode will depend on the D2D receivers which are on the minor arc of the overlapping circle of $b(y, R_d)$.

Lemma 3: Conditioned on primary user x_o at the origin with a guard zone of radius R_{GZ}, the intensity measure of D2D transmitters y that can operate in the half-duplex mode will be,

$$\Lambda_{HD} = \int_{R_{GZ}}^{R_{GZ}+R_d} \lambda_d \zeta_{min}\left(R_{GZ}, R_d, r_{x_o,y}\right) r dr. \tag{15}$$

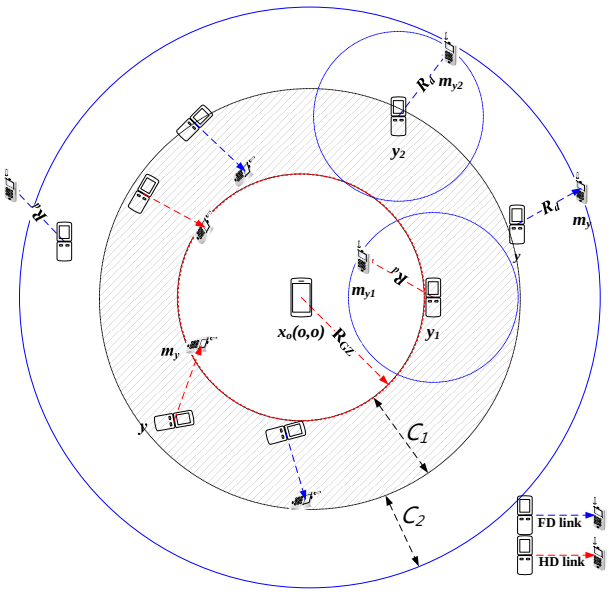

FIGURE 4: An area of interest where D2D communication link can be either in half-duplex or full-duplex mode depending on the angle (θ) of the receiver (m_y)

Proof: Proof is given in Appendix VIII-C.

The expression for ζ_{min} is given in Eq. 14. Based on this, we can derive the probability of D2D links to be half-duplex mode next.

Lemma 4: Given the intensity measure of D2D users in the half-duplex mode as Λ_{HD}, the probability of the half-duplex mode will be,

$$p_{HD} = \frac{\Lambda_{HD}}{2\pi R_p^2} \tag{16}$$

Proof: The probability of half-duplex users is derived by getting the ratio of half-duplex users (Λ_{HD}) by a total number of D2D users in a given area of interest i.e. total area (πR_p^2). This has further been validated and results are shown in Fig. 7b.

C. CASE 3: D2D PAIR OUTSIDE GZ FULL-DUPLEX MODE

In this case, a D2D communication pair can share a primary user's spectrum without disrupting its reception. D2D links can operate in the FD mode in two regions, the transmitters and receivers in region $\mathcal{C}_1$, whose receivers are on the major arc of the overlap circles (i.e. outside GZ) and D2D transmitters and receivers in region $\mathcal{C}_2 = b(o, R_{GZ} + R_d)^c$. Depending on the distance of D2D transmitters (y) and receivers (m_y), distance based conditions for D2D users operating in FD mode in regions $\mathcal{C}_1$ and $\mathcal{C}_2$ can be expressed as,

$$\begin{cases} R_{GZ} < r_{x_o,y} < R_{GZ} + R_d & y, m_y \in \mathcal{C}_1 \\ r_{x_o,y} \geq R_{GZ} + R_d & y, m_y \in \mathcal{C}_2. \end{cases}$$

This mechanism of mode selection in turn significantly increases the areal spectral efficiency of SUs as the D2D pairs can use full-duplex capability while protecting the reception of primary users. Since the induced interference from a FD receiver will not disrupt the primary user's transmission, so it can harvest the data-rate gains of FD communication. To characterize the interference field of FD D2D users, we have to consider the interference generated by D2D users in two regions, $\mathcal{C}_1$ and $\mathcal{C}_2$. In terms of the indicator function, we can formulate the counting measure of FD transmitters as,

$$\Lambda_{FD} = \sum_{y_i \in \varphi_d} \mathbb{1}_{(R_{GZ}+R_d < ||Y_i|| \leq \infty)} + \sum_{y_i \in \varphi_d} \mathbb{1}_{(R_{GZ} < ||Y_i|| \leq R_{GZ}+R_d)} \mathbb{1}_{(R_{GZ} < ||m_{Y_i}|| \leq R_{GZ}+R_d)} \tag{17}$$

The intensity of D2D transmitters in region $\mathcal{C}_2$ is comparatively easier to formulate, however, the intensity of FD D2D users in region $\mathcal{C}_1$ requires the angle of the major arc of an overlapping circle. Since we have the intensity measure of the D2D transmitters operating in the HD mode, now, the receivers of D2D transmitters which will be outside R_{GZ} will be on the major arc of circle $b(y, R_d)$. As, the total angle of a circle is 2π, the probability of a D2D communication link in

This article has been accepted for publication in a future issue of this journal, but has not been fully edited. Content may change prior to final publication. Citation information: DOI 10.1109/ACCESS.2019.2913538, IEEE Access

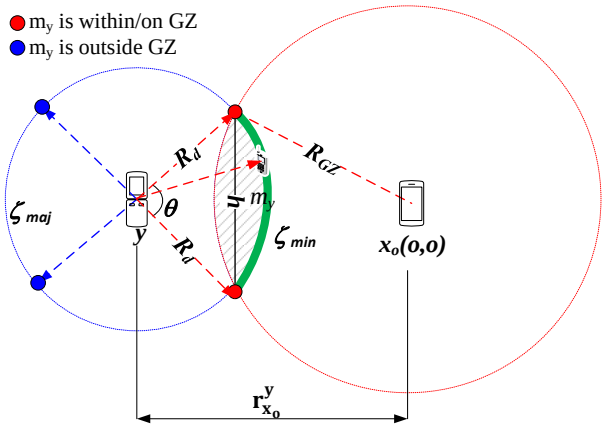

FIGURE 5: Location of D2D receiver will either be on the length of the minor arc ζ_{min} (green) or on major arc ζ_{maj} (blue)

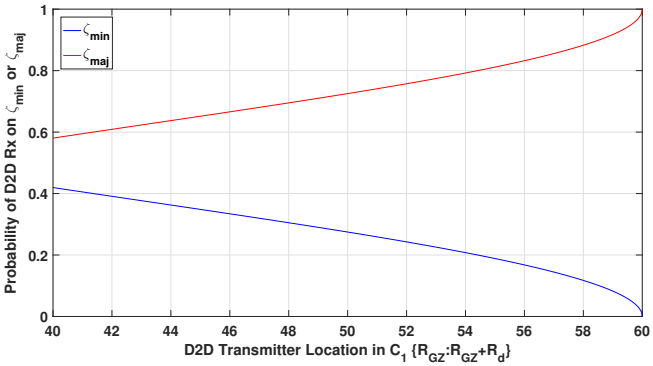

FIGURE 6: Probability of D2D receiver to be located on either ζ_{min} (HD mode) or on ζ_{maj} (FD mode) as a function of distance of D2D Tx in $\mathcal{C}_1$

this scenario where D2D Rx will be on major arc ζ_{maj} (i.e. green arc in Fig. 5) is given by:

$$\zeta_{maj} = (2\pi - \theta)R_d. \tag{18}$$

where, θ is given in VIII-B as an angle of a receiver with its D2D transmitter, when RX exists on minor arc and operates in the half-duplex mode. Now, the intensity measure of D2D transmitters operating in the FD mode within $\mathcal{C}_1$ with receivers located on the major arc of $b(y, R_d)$ is denoted by $\tilde{\Lambda}_{FD}$,

$$\tilde{\Lambda}_{FD} = 2\lambda_d \int_{R_{GZ}}^{R_{GZ}+rd} (2\pi - \theta(y, R_d, R_{GZ}))\, ydy. \tag{19}$$

Thus, the total intensity measure of the D2D transmitters that can operate in full duplex mode can be expressed as the sum of the counting measures of D2D transmitters in regions $\mathcal{C}_1$ and $\mathcal{C}_2$,

$$\Lambda_{FD} = 2\lambda_d \int_{R_{GZ}}^{R_{GZ}+rd} (2\pi - \theta(y, R_d, R_{GZ}))\, ydy + 2\pi\lambda_d \int_{R_{GZ}+R_d}^{\infty} ydy. \tag{20}$$

Hence, the probability of these transmitters to be in the FD mode will simply be a normalization of Λ_{FD} over $|A|$, given in VIII-D.

Lemma 5: Conditioned on the circular disk of radius $R_{GZ} + R_d$ at origin o, the probability of a D2D communication link to be in the full-duplex mode in regions $\mathcal{C}_1$ and $\mathcal{C}_2$ can be expressed as,

$$p_{FD} = \frac{2\pi\lambda_d}{|A|}\left(|A| - \pi(R_{GZ} + R_d)^2\right). \tag{21}$$

Proof: Proof is given in Appendix VIII-D, corresponding analytical and simulation results are presented in Fig. 7c. As shown, with the increase in interference protection for cellular user (R_{GZ}), the probability of FD tends to decrease as it eventually decreases the interference from a D2D link by putting more links to either silent or half-duplex mode. Also, p_{FD} is less for higher D2D link distances (R_d) as this yields more D2D links to be in the half-duplex mode in region $\mathcal{C}_1$.

Probability of D2D Rx to be on ζ_{maj} or ζ_{maj}: The pdf of angle θ between D2D Tx and D2D Rx is $1/2\pi$. The probability of D2D Rx to located on either $\zeta_{maj} or \zeta_{maj}$ arc is shown in Fig. 6 as a function of D2D Tx distance in $\mathcal{C}_1$. As the transmitter moves away from GZ the probability of D2D link to be in FD mode increases which is shown with the increase of ζ_{maj}. On the other hand, if the D2D Tx is in the vicinity of GZ, then the probability of link to operate in HD mode (Rx on ζ_{min}) is higher which also ensures protection to primary receiver.

As we have now the relative intensities for D2D transmitters in a half-duplex and full-duplex mode so we can assess the interference from these users to primary users when computing the success probability. The interference field for a typical user from full-duplex links will be twice that of Λ_{FD} because of the receivers of active full-duplex D2D links. Hence, the trade-off between capacity of active full-duplex D2D transmitters Λ_{FD}, and protection for a cellular receiver based on guard-zone radius (R_{GZ}) is an interesting optimization problem to consider.

V. SUCCESS PROBABILITY AND SIR ANALYSIS

In this section, we characterize the complementary cumulative distribution function (CCDF) of SIR, which is also known as a complement of the outage probability that can equally be thought of as the average fraction of the network area or users to achieve the target SIR threshold T. The success probability of a typical user is expressed in terms of the Laplace transform of aggregate interference as the channel gains for interfering users follow Rayleigh fading with an exponential distribution i.e. $\exp(\mu)$. The SIR success probability is a key parameter which is used to further evaluate expressions for the data rate, throughput and Area Spectral Efficiency (ASE). The success probability of a typical user

This article has been accepted for publication in a future issue of this journal, but has not been fully edited. Content may change prior to final publication. Citation information: DOI 10.1109/ACCESS.2019.2913538, IEEE Access

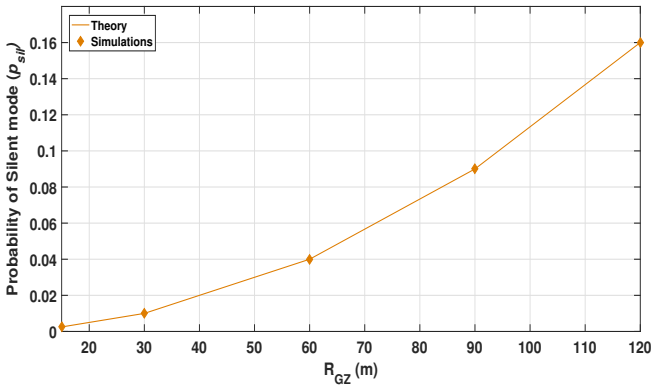

(a) Probability of Silent D2D links as function of R_{GZ} from Lemma 1 and simulations

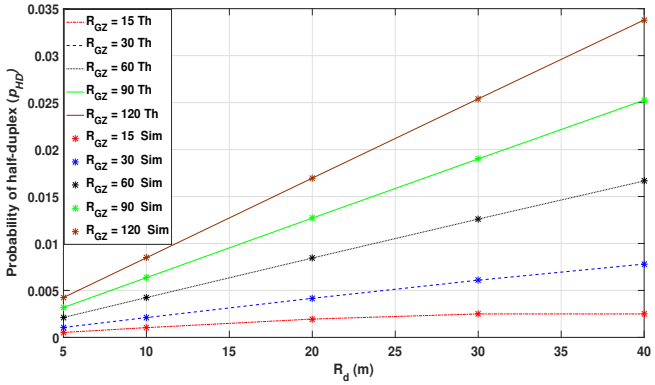

(b) Probability of half-duplex D2D links from Lemma 4 as a function of R_{GZ} and R_d with simulation results

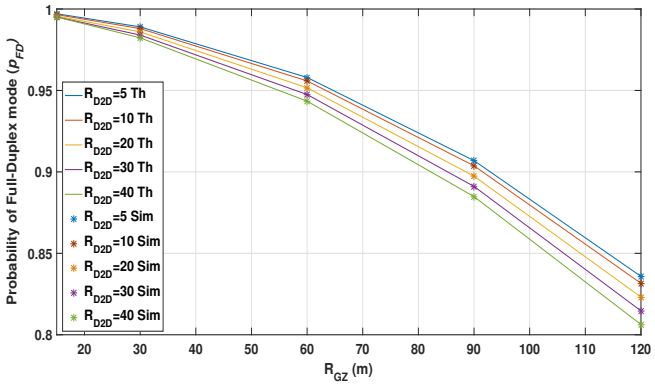

(c) Probability of full-duplex D2D links as a function of R_{GZ} and R_d from Lemma 5 and simulations

FIGURE 7: Probability of D2D links to be in Silent, Half-Duplex and Full-Duplex mode as a function of R_{GZ} and R_d

under consideration is given in section III-C.

Approximation: Due to sophisticated mathematical derivation for expressions of success probability and loss of analytical tractability, the φ_d is approximated to Φ_d with the hole carved out at origin $b(o, R_{GZ})$. The intensity of D2D transmitters and receivers is represented with λ_d for notational simplicity. For simplicity of analysis, as we have considered single cellular user so, we assume one hole in the PHP and approximate it to PPP beyond that hole, also been done in previous works for similar reasons. The point processes for different users are assumed to be independent of each other to provide the abstract level analysis of the proposed method.

A. SIR SUCCESS PROBABILITY OF CELLULAR USER

To formulate the success probability of a typical cellular user (x_o) in downlink, we consider a receiver at the origin connected to the base station at distance of R_c with interference protection provided through a circular guard-zone of radius R_{GZ}. The interference field for a typical receiver constitutes of all of the D2D active users in a cell except the tagged base station. As discussed in section IV, conditioned on the critical regions and parameters ($\mathcal{C}_1$, $\mathcal{C}_2$, and $\theta(y, m_y)$), the interference field consists of D2D transmitters in the half-duplex mode (Λ_{HD}) , D2D transmitters ($\Lambda_{FD}(y)$) and receivers ($\Lambda_{FD}(m_y)$) in the full-duplex mode. From 15 and 20, we can write the interference field for (x_o) as,

$$\Lambda_{IF}^{x_o} = \Lambda_{HD} + \Lambda_{FD}(y) + \Lambda_{FD}(m_y). \tag{22}$$

Equipped with the counting measures of interfering users, we can now formulate the success probability of a typical cellular user.

Proposition 1: In a considered network, the success probability of a typical cellular receiver is the Laplace transform of interference from half-duplex and full-duplex D2D users, which is given by,

$$p_s^{x_o} = \exp(-2\pi\lambda_d \mathcal{H}(\theta, R_d, \alpha_d)) \exp(-2\pi\lambda_d \mathcal{F}_T(\theta, R_d, \alpha_d)) \exp(-2\pi\lambda_{m_d} \mathcal{F}_R(\theta, R_d, \alpha_d)) \tag{23}$$

where,

$$\mathcal{H}(\theta, R_d, \alpha_d) = \int_{R_{GZ}}^{R_{GZ}+R_d} \frac{\theta(y, R_d, R_{GZ})}{2\pi(1 + \frac{||y||^{\alpha_d}}{s})} y dy, \tag{24}$$

$$\mathcal{F}_T = \int_{R_{GZ}}^{R_{GZ}+R_d} \frac{2\pi - \theta(y, R_d, R_{GZ})}{2\pi(1 + \frac{||y||^{\alpha_d}}{s})} y dy + \int_{R_{GZ}+R_d}^{\infty} \frac{1}{1 + \frac{||y||^{\alpha_d}}{s}} y dy, \tag{25}$$

$$\mathcal{F}_R = \int_{R_{GZ}}^{R_{GZ}+R_d} \frac{2\pi - \theta(m_y, R_d, R_{GZ})}{2\pi(1 + \frac{||m_y||^{\alpha_d}}{s})} m_y dm_y + \int_{R_{GZ}+R_d}^{\infty} \frac{1}{1 + \frac{||m_y||^{\alpha_d}}{s}} m_y dm_y, \tag{26}$$

and,

$$s = \frac{T R_c^{\alpha_c} P_d}{P_c} \tag{27}$$

Proof: The success probability can be expressed by putting Eq. 7 in Eq. 6,

$$p_s^{x_o} = F^c_{x_o, x_{BS}} > T \frac{\mathcal{I}_{x_o, y} + \mathcal{I}_{x_o, m_y}}{P_c l\,(x_o, x_{BS})} \tag{28}$$

This article has been accepted for publication in a future issue of this journal, but has not been fully edited. Content may change prior to final publication. Citation information: DOI 10.1109/ACCESS.2019.2913538, IEEE Access

where, $l\left(x_o, x_{BS}\right)$ is the path-loss of a typical user to its tagged base station. $\mathcal{I}_{x_o,y}$ is the interference field from all the active D2D transmitters (both in HD and FD mode),

$$\mathcal{I}_{x_o,y} = \sum_{y\epsilon\Phi_d} P_d F^d_{x_o,y} l(o,y) 1^{HD}_{m_y,y} + \sum_{y\epsilon\Phi_d} P_d F^d_{x_o,y} l(o,y) 1^{FD}_{m_y,y}, \tag{29}$$

Also, $\mathcal{I}_{x_o,m_y}$ is the interference from D2D Rxs conditioned on the links in the FD mode,

$$\mathcal{I}_{x_o,m_y} = \sum_{m_y\in\Phi_{m_d}} P_d F^d_{x_o,m_y} l(x_o,m_y) 1^{FD}_{m_y,y} \tag{30}$$

Expressing the constants in Eq. 28 with s as in Eq. 27. The total interference experienced by typical PU (x_o) is originated from three set of users as expressed in Eqs. 29 and 30. The Laplace transform of these interference terms follows as,

$$\begin{aligned}\mathcal{L}_{\mathcal{I}}(s) = \mathbb{E}_{\Phi_d,\Phi_{m_d},\theta(HD/FD)} & \left(\prod_{y\epsilon\Phi_d} \exp(-sF^d_{x_o,y} l(o,y) 1^{HD}_{m_y,y})\right) \\ & \left(\prod_{y\epsilon\Phi_d} \exp(-sF^d_{x_o,y} l(o,y)) 1^{FD}_{m_y,y}\right) \\ & \left(\prod_{y\epsilon\Phi_{m_d}} \exp(-sF^d_{x_o,m_y} l(o,m_y)) 1^{FD}_{m_y,y}\right)\end{aligned} \tag{31}$$

Relaxing the inter-dependencies of the point processes we will now characterize the Laplace transform of these terms individually. First, considering the interference from HD D2D transmitters,

$$\mathcal{L}_1(s) = \mathbb{E}_{\Phi_d,HD}\left(\prod_{y\epsilon\Phi_d} exp(-sF^d_{x_o,y} l(o,y) 1^{HD}_{m_y,y})\right) \tag{32}$$

Applying Rayleigh channel distribution (i.e. $F^d_{x_o,y} \sim exp(\mu)$), the PGFL of PPP and conventional stochastic geometry machinery,

$$\mathcal{L}_1(s) = \mathbb{E}_{HD}\left(\int_{\mathbb{R}^2\setminus b(o,R_{GZ})} \frac{1}{1+\frac{||y||^{\alpha_d}}{s}} y dy 1^{HD}_{m_y,y}\right) \tag{33}$$

As the segregation between HD and FD D2D links is based on angle θ between transmitter and receiver located inside region $\mathcal{C}_1$, we can express the expectation of a transmitter being in the HD mode as,

$$\begin{aligned}\mathbb{E}_{HD}\left\{1^{HD}_{m_y,y}\right\} = \mathbb{E}_{HD}\{ & \mathbb{1}_{(R_{GZ}<||y||\leq R_{GZ}+R_d)} \\ & \mathbb{1}_{||m_y||<R_{GZ}}\}.\end{aligned} \tag{34}$$

Similarly, the expectation measure for D2D transmitters and receivers in the full-duplex mode will be,

$$\begin{aligned}\mathbb{E}_{FD}\left\{1^{FD}_{m_y,y}\right\} = \mathbb{E}_{FD}\{ & \mathbb{1}_{(R_{GZ}<||y||\leq R_{GZ}+R_d)} \cdot \\ & \mathbb{1}_{(R_{GZ}<||m_y||<R_{GZ}+R_d)} + \mathbb{1}_{(R_{GZ}+R_d<||y||\leq\infty)} \cdot \\ & \mathbb{1}_{(R_{GZ}+R_d<||m_y||\leq\infty)}\}.\end{aligned} \tag{35}$$

These distance based expectation measures can be applied as pdf of the angle (θ) between D2D transmitter and receiver as explained in section IV. The pdf of the θ for HD and FD links in $\mathcal{C}_1$ will be,

$$f_{HD}(\theta) = \frac{\theta(y,R_d,R_{GZ})}{2\pi} \tag{36}$$

$$f_{FD}(\theta) = \frac{2\pi - \theta(y,R_d,R_{GZ})}{2\pi} \tag{37}$$

Applying the expectation for HD in Eq. 33 with the pdf of f_{HD}, and converting into polar coordinates,

$$\mathcal{L}_1(s) = \exp\left(-2\pi\lambda_d \int_{R_{GZ}}^{R_{GZ}+R_d} \frac{f_{HD}(\theta)}{1+\frac{||y||^{\alpha_d}}{s}} y dy\right) \tag{38}$$

The inside integral term is denoted by $\mathcal{H}(\theta,R_d,\alpha_d)$. Now, the second interference terms in Eq. 31 consists of FD interferers in regions $\mathcal{C}_1$ and $\mathcal{C}_2$. Since, all D2D transmitters in $\mathcal{C}_2$ can communicate in FD mode so its Laplace transform will be easier to compute. However, for FD users inside $\mathcal{C}_1$ are conditioned on the angle θ of the major arc. Thus, for the FD transmitters in $\mathcal{C}_1$, the pdf of $f_{FD}(\theta)$ will be applied to incorporate the probability of FD mode. Using the standard simplification machinery, the Laplace transform of second term in Eq. 31 will be ,

$$\begin{aligned}\mathcal{L}_2(s) = \exp\Bigg(-2\pi\lambda_d \Bigg(& \int_{R_{GZ}}^{R_{GZ}+R_d} \frac{f_{FD}(\theta)}{1+\frac{||y||^{\alpha_d}}{s}} y dy + \\ & \int_{R_{GZ}+R_d}^{\infty} \frac{1}{1+\frac{||y||^{\alpha_d}}{s}} y dy\Bigg)\Bigg)\end{aligned} \tag{39}$$

Similarly, the Laplace transforms of third interference terms in Eq. 31 can be written as,

$$\begin{aligned}\mathcal{L}_3(s) = \exp\Bigg(-2\pi\lambda_{m_d} \Bigg(& \int_{R_{GZ}}^{R_{GZ}+R_d} \frac{f_{FD}(\theta)}{1+\frac{||m_y||^{\alpha_d}}{s}} m_y dm_y \\ & + \int_{R_{GZ}+R_d}^{\infty} \frac{1}{1+\frac{||m_y||^{\alpha_d}}{s}} m_y dm_y\Bigg)\Bigg)\end{aligned} \tag{40}$$

The inside integrals in $\mathcal{L}_2(s)$ and $\mathcal{L}_3(s)$ are denoted by $\mathcal{F}_T(\theta,R_d,\alpha_d)$ and $\mathcal{F}_R(\theta,R_d,\alpha_d)$, respectively. Inserting expressions for $f_{HD}(\theta)$ and $f_{FD}(\theta)$ completes the proof.

VI. RESULTS AND ANALYSIS

In this section, performance analysis of both cellular and D2D network is done using the system model given in section III. Monte-carlo simulations have been used with a large number of iterations and randomness to get the average of

This article has been accepted for publication in a future issue of this journal, but has not been fully edited. Content may change prior to final publication. Citation information: DOI 10.1109/ACCESS.2019.2913538, IEEE Access

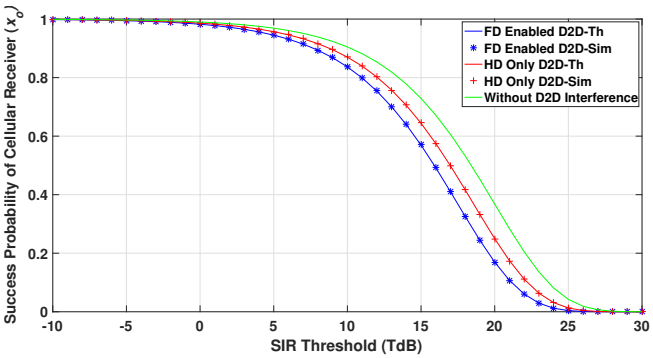

FIGURE 8: Success probability of typical cellular receiver as a function of SIR threshold. System configuration parameters are λ_d=0.002, P_c=50dBm, P_d=80dBm, α_d=4

performance metric for either the cellular or D2D receiver at the origin. The simulation values of the network configuration parameters are listed in Table 2, unless mentioned elsewhere specifically. The probability of success for typical cellular or D2D user is evaluated against SIR threshold (TdB) and plotted in result figures.

Fig. 8 shows preliminary theoretical and simulation results for success probability of a typical cellular user with FD enabled D2D secondary users, HD only D2D users and without any D2D users. As shown, with FD enabled D2D users the success probability drops at the cost of improved gains for secondary users. This trade-off needs extensive and further critical analysis to assess the FD gains for secondary users in cognitive networks. Further simulation results are presented in next section.

Success Probability of Cellular User: An interesting result presented in Fig. 9a shows the impact of increasing the D2D user intensity over success probability of a typical cellular receiver. As, the intensity (λ_D) of D2D users increases, it increases the probability of full-duplex users, hence, contributing more interference for a cellular receiver. This factor causes a gradual decrease in success probability of cellular receiver as shown in Fig. 9a. From λ_D 0.001 to 0.5, a typical cellular receiver experiences aggressive interference from D2D users in the half-duplex and full-duplex modes. The key factor in the decline of success probability is the interference from both D2D transmitters and receivers

TABLE 2: Simulation Parameters and their values

Parameter	Simulation Values
λ_d	$\{0.001, 0.005, 0.05, 0.5\} Users/Km^2$
$F_{o,\kappa}$	μ
α_c, α_d	4, 3.7
P_c, P_d	0.6,0.4
β	0.3
T	-20:1:20
R_{GZ}	$\{15, 30, 60, 90\} m$
R_d	$\{10, 20, 30\} m$
R_c	$\{4, 6\} m$

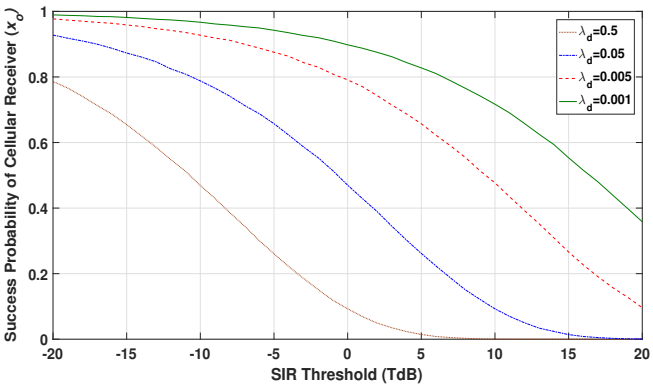

(a) Success probability of a cellular receiver as a function of SIR threshold (TdB) for different λ_D

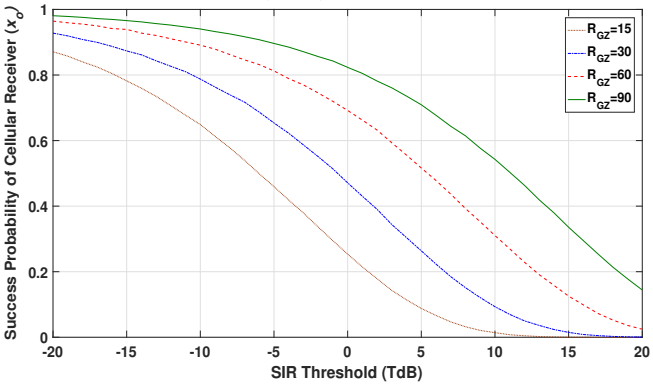

(b) Success probability of a cellular receiver as a function of SIR threshold (TdB) for different R_{GZ}

FIGURE 9: Success probability of typical cellular receiver ($p_s^{x_o}$) as a function of λ_D and R_{GZ}

operating in the full-duplex mode. Therefore, a trade-off between success probability and a number of active D2D users is another interesting research direction which will be explored in the future. The critical parameter R_{GZ} controls the capacity of active D2D links and also protects the cellular user's reception. As shown in Fig. 9b, a greater guard zone protects cellular users reception from D2D interference by putting more D2D links in the silent mode. Thus, a higher guard zone protection guarantees a higher success probability for a typical cellular user, whereas, a smaller guard zone results in an increased interference field from half-duplex transmitters and full-duplex transmitters/receivers, resulting in a lower success probability of cellular receiver.

Success Probability of D2D User: The simulation results for the success probability of a typical D2D receiver as a function of R_{GZ} and R_d is shown in Fig. 10a and 10b, respectively. The typical link is operating in HD mode. As R_{GZ} increases, the success probability of the D2D link also increases due to the fact that a higher guard zone protection results in a reduced interference field from active D2D users. Another factor is a distance of the cellular receiver from a typical D2D link as if it is in the vicinity then it will put the dominant D2D interferes in the silent mode. Therefore,

This article has been accepted for publication in a future issue of this journal, but has not been fully edited. Content may change prior to final publication. Citation information: DOI 10.1109/ACCESS.2019.2913538, IEEE Access

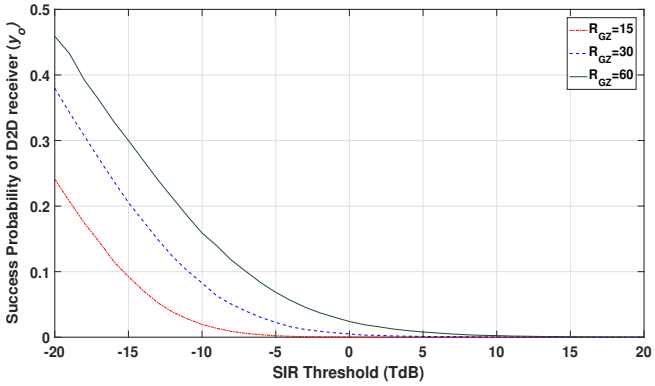

(a) Success probability of a D2D receiver as a function of SIR threshold (TdB) for different R_{GZ}

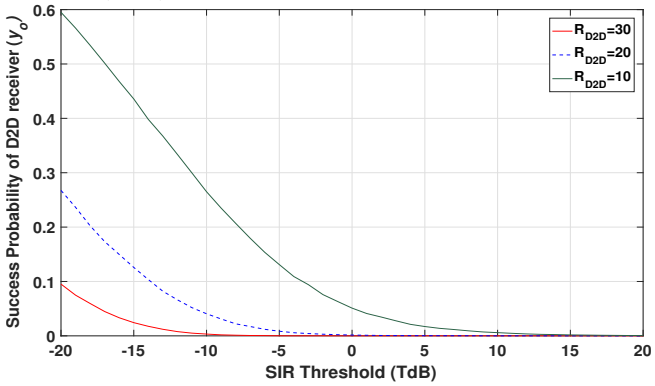

(b) Success probability of a D2D receiver as a function of SIR threshold (TdB) for different R_d

FIGURE 10: Success probability of typical D2D receiver in HD mode as function of R_{GZ} and R_d.

the optimal size of the guard zone balances the performance trade-off between the success probability of cellular and D2D users. Another critical factor affecting the performance of the success probability of a typical D2D link is the D2D link distance (R_d) as shown in Fig. 10b. As R_d increases, the success probability decreases due to the fact that this will result in an increase in half-duplex D2D links rather than the full-duplex D2D links. So, the interference field will contain more HD transmitters rather than FD transmitters and receivers, hence, less interference with higher R_d. This is in correlation with the overlap area shown in Fig. 4, decreasing the probability of the full-duplex D2D links.

VII. CONCLUSION AND FUTURE WORK

In this work, we have presented a comprehensive analysis of cognitive network where primary user's reception are protected with guard zones from full-duplex enabled D2D secondary users. Using stochastic geometry tools, the impact of D2D users in the vicinity of active cellular user is studied. We defined a critical region where D2D link can operate in half-duplex mode if D2D receiver is inside the guard zone and can operate in full-duplex mode if both D2D transmitter and receiver is outside. The probabilities of half duplex and full duplex modes are derived and validated through extensive simulation results. The interference to primary user is also characterized from active D2D links in half duplex and full duplex modes. From preliminary analysis and results, it is possible to allow secondary users in cognitive setup to harvest the gains of full duplex technology as long as the primary user is guaranteed certain interference protection. The trade-off between D2D network capacity and its impact on success probability of a cellular user is also studied and results are presented. One of the interesting extensions of this work is to find an optimum guard-zone radius which can provide maximum D2D user capacity. Further analysis is also possible by considering multiple concurrent cellular users reception and how it affects the D2D network capacity.

VIII. APPENDIX

A. PROBABILITY OF SILENT MODE

Assuming points are uniformly and randomly distributed by PPP. Let $|A|$ be the total area/bounded set ($|A| < \infty$) of the plane where all D2D points are distributed with intensity λ_d. Also, B is a circular disk of radius R_{GZ} at origin (o), then the probability of D2D points being in $B \subset A$ will be,

$$p_{sil}\left(y \in B\right) = \frac{|B|}{|A|} \tag{41}$$

Now, the expected intensity measure of points in B will be ,

$$\begin{aligned}\mathbb{E}\left\{\Lambda_{|B|}\right\} &= \mathbb{E}\left[\sum_{y_i \in \Phi_d} \mathbb{1}_{(0<||Y_i||\leq R_{GZ})}\right] \\ &\overset{a}{=} \lambda_d \int_0^{\infty}\int_0^{2\pi} \mathbb{1}_{(0<||y_i||\leq R_{GZ})} d\theta dr \\ &\overset{b}{=} 2\pi\lambda_d \int_0^{R_{GZ}} r dr = \pi\lambda_d R_{GZ}^2. \end{aligned} \tag{42}$$

where (a) is derived from Campbell's theorem for PPP and (b) from applying the integrals for polar coordinates. Putting it into $p_{sil}\left(y \in B\right)$ completes the proof.

B. CHORD LENGTH

Assuming typical receiver at the origin (o, o), with guard zone circular disk of radius R_{GZ} and D2D transmitter at distance of $r^y_{x_o}$. We are interested to calculate the minor arc length shown in Fig. 5 as ζmin. First, we have to find out the the angle θ, for which we need $h/2$ as shown in the figure. From trigonometry and basic circular geometry, the arc length can be found using the following formula depending on the known parameters [33],

$$\zeta_{min} = R_d\theta,$$

Now, h is,

$$h = \frac{1}{r^y_{x_o}}\sqrt{4{r^y_{x_o}}^2 R_{GZ}^2 - \left({r^y_{x_o}}^2 - R_d^2 + R_{GZ}\right)^2}, \tag{43}$$

while θ, is

$$\theta(r^y_{x_o}, R_d, R_{GZ}) = 2\arcsin\left(\frac{h}{2R_d}\right). \tag{44}$$

So, the length of the minor arc will be ,

$$\zeta_{min} = 2R_d \arcsin\left(\frac{\sqrt{4{r^y_{x_o}}^2 R^2_{GZ} - \left({r^y_{x_o}}^2 - R^2_d + R_{GZ}\right)^2}}{2R_d r^y_{x_o}}\right). \tag{45}$$

C. D2D TX IN HD MODE

From VIII-B, we can segregate the D2D transmitters y and receivers m_y, which will communicate in the half-duplex mode based on the angle θ or if it lies on ζ_{min}. Now, to calculate the total number of D2D Txs in regions $\mathcal{C}_1$ whose receivers are on ζ_{min}, denoted by subset $|B|$, we have:

$$\mathbb{E}\left\{\Lambda_{|B|}\right\} = \mathbb{E}\left[\sum_{y_i \in \Phi_d} \mathbb{1}_{(R_{GZ} < ||Y_i|| \leq R_{GZ}+R_d)} . \mathbb{1}_{(\theta_{m_{Y_i}} = \zeta_{min})}\right] \tag{46}$$

From the application of Campbell theorem, after applying the integrals and converting to polar coordinates we will have the total intensity of users in $|B|$,

$$\lambda_{HD} = \int_{R_{GZ}}^{R_{GZ}+rd} r\lambda_d \zeta_{min} dr. \tag{47}$$

Putting in the expression for ζ_{min} completes the proof.

D. PROBABILITY OF FULL DUPLEX MODE

To account for a D2D transmitter that will communicate in the full-duplex mode, we have to find the number of transmitters that can communicate in the full-duplex mode in two regions $\mathcal{C}_1$ and $\mathcal{C}_2$. This, includes all the transmitters of $\mathcal{C}_2$ $R_{GZ} + R_d < ||y|| < \infty$. Considering subset $B \subset A$, where, $B = \mathcal{C}_1 \cup \mathcal{C}_1$, and following the same steps as in VIII-A, the expected counting measure of D2D transmitters in $\mathcal{C}_1$,

$$\mathbb{E}\left\{\Lambda_{\mathcal{C}_1}\right\} = 2\pi\lambda_d \int_{R_{GZ}}^{R_{GZ}+R_d} y dy \tag{48}$$

Similarly, for counting measure of D2D transmitters in $\mathcal{C}_2$,

$$\mathbb{E}\left\{\Lambda_{\mathcal{C}_2}\right\} = 2\pi\lambda_d \int_{R_{GZ}+R_d}^{\infty} y dy \tag{49}$$

From 41, the probability of D2D links to be in the full-duplex mode will be,

$$p_{FD}\left(y \in B\right) = \frac{\Lambda_{\mathcal{C}_1} + \Lambda_{\mathcal{C}_2}}{\Lambda_{|A|}} \tag{50}$$

Inserting the expressions for the intensity measures into above equation, we can have the equation for p_{FD}.

REFERENCES

[1] Y. Wang, J. Li, L. Huang, Y. Jing, A. Georgakopoulos, and P. Demestichas, "5G mobile: Spectrum broadening to higher-frequency bands to support high data rates," IEEE Vehicular technology magazine, vol. 9, no. 3, pp. 39–46, 2014.

[2] J. M. Peha, "Approaches to spectrum sharing," IEEE Communications magazine, vol. 43, no. 2, pp. 10–12, 2005.

[3] S. Yrjölä, P. Ahokangas, and M. Matinmikko, "Evaluation of recent spectrum sharing concepts from business model scalability point of view," in Dynamic Spectrum Access Networks (DySPAN), 2015 IEEE International Symposium on, pp. 241–250, IEEE, 2015.

[4] I. F. Akyildiz, W.-Y. Lee, M. C. Vuran, and S. Mohanty, "Next generation/dynamic spectrum access/cognitive radio wireless networks: A survey," Computer Networks, vol. 50, no. 13, pp. 2127 – 2159, 2006.

[5] I. F. Akyildiz, S. Nie, S.-C. Lin, and M. Chandrasekaran, "5G roadmap: 10 key enabling technologies," Computer Networks, vol. 106, pp. 17–48, 2016.

[6] J. G. Andrews, S. Buzzi, W. Choi, S. V. Hanly, A. Lozano, A. C. Soong, and J. C. Zhang, "What will 5G be?," IEEE Journal on selected areas in communications, vol. 32, no. 6, pp. 1065–1082, 2014.

[7] Y. Mehmood, N. Haider, M. Imran, A. Timm-Giel, and M. Guizani, "M2M Communications in 5G: State-of-the-Art Architecture, Recent Advances, and Research Challenges," IEEE Communications Magazine, vol. 55, pp. 194–201, Sep. 2017.

[8] Z. Zhang, X. Chai, K. Long, A. V. Vasilakos, and L. Hanzo, "Full duplex techniques for 5G networks: self-interference cancellation, protocol design, and relay selection," IEEE Communications Magazine, vol. 53, no. 5, pp. 128–137, 2015.

[9] K. S. Ali, H. ElSawy, M.-S. Alouini, A. Khavasi, and J. Suk, "Modeling Cellular Networks With Full-Duplex D2D Communication: A Stochastic Geometry Approach," IEEE Transactions on Communications, vol. 64, no. 10, p. 4409, 2016.

[10] S. Kim and W. Stark, "Full duplex device to device communication in cellular networks," in Computing, Networking and Communications (ICNC), 2014 International Conference on, pp. 721–725, IEEE, 2014.

[11] K. T. Hemachandra, N. Rajatheva, and M. Latva-aho, "Sum-rate analysis for full-duplex underlay device-to-device networks," in Wireless Communications and Networking Conference (WCNC), 2014 IEEE, pp. 514–519, IEEE, 2014.

[12] S. Ali, N. Rajatheva, and M. Latva-aho, "Full duplex device-to-device communication in cellular networks.," in EuCNC, pp. 1–5, 2014.

[13] H. Chen, L. Liu, H. S. Dhillon, and Y. Yi, "QoS-Aware D2D Cellular Networks with Spatial Spectrum Sensing: A Stochastic Geometry View," IEEE Transactions on Communications, 2018.

[14] M. Naslcheraghi, M. Afshang, and H. S. Dhillon, "Modeling and performance analysis of full-duplex communications in cache-enabled d2d networks," in 2018 IEEE International Conference on Communications (ICC), pp. 1–6, IEEE, 2018.

[15] M. Haenggi, J. G. Andrews, F. Baccelli, O. Dousse, and M. Franceschetti, "Stochastic geometry and random graphs for the analysis and design of wireless networks," IEEE Journal on Selected Areas in Communications, vol. 27, no. 7, pp. 1029–1046, 2009.

[16] K. Khan and A. Jamalipour, "Coverage Analysis for Multi-Request Association Model (MRAM) in a Caching Ultra-Dense Network," IEEE Transactions on Vehicular Technology, pp. 1–1, 2019.

[17] J. G. Andrews, A. K. Gupta, and H. S. Dhillon, "A primer on cellular network analysis using stochastic geometry," arXiv preprint arXiv:1604.03183, 2016.

[18] H. ElSawy, E. Hossain, and M. Haenggi, "Stochastic geometry for modeling, analysis, and design of multi-tier and cognitive cellular wireless networks: A survey," IEEE Communications Surveys & Tutorials, vol. 15, no. 3, pp. 996–1019, 2013.

[19] J. Lee and T. Q. Quek, "Device-to-device communication in wireless mobile social networks," in Vehicular Technology Conference (VTC Spring), 2014 IEEE 79th, pp. 1–5, IEEE, 2014.

[20] N. T. Viet and F. Baccelli, "Stochastic modeling of carrier sensing based cognitive radio networks," in Modeling and Optimization in Mobile, Ad Hoc and Wireless Networks (WiOpt), 2010 Proceedings of the 8th International Symposium on, pp. 472–480, IEEE, 2010.

[21] J. G. Andrews, F. Baccelli, and R. K. Ganti, "A tractable approach to coverage and rate in cellular networks," IEEE Transactions on communications, vol. 59, no. 11, pp. 3122–3134, 2011.

[22] A. Ali and A. Hasan, "Stochastic geometry of thinned nodes in ad hoc networks," in Applied Sciences and Technology (IBCAST), 2012 9th International Bhurban Conference on, pp. 431–435, IEEE, 2012.

[23] H. S. Dhillon, R. K. Ganti, F. Baccelli, and J. G. Andrews, "Modeling and analysis of K-tier downlink heterogeneous cellular networks," IEEE Journal on Selected Areas in Communications, vol. 30, no. 3, pp. 550–560, 2012.

This article has been accepted for publication in a future issue of this journal, but has not been fully edited. Content may change prior to final publication. Citation information: DOI 10.1109/ACCESS.2019.2913538, IEEE Access

[24] C.-h. Lee and M. Haenggi, "Interference and outage in poisson cognitive networks," IEEE Transactions on Wireless Communications, vol. 11, no. 4, pp. 1392–1401, 2012.

[25] P. Parida, H. S. Dhillon, and P. Nuggehalli, "Stochastic geometry-based modeling and analysis of citizens broadband radio service system," IEEE Access, vol. 5, pp. 7326–7349, 2017.

[26] A. Hasan and A. Ali, "Guard zone-based scheduling in ad hoc networks," Computer Communications, vol. 56, pp. 89 – 97, 2015.

[27] Y. Li, F. Baccelli, J. G. Andrews, T. D. Novlan, and J. C. Zhang, "Modeling and Analyzing the Coexistence of Wi-Fi and LTE in Unlicensed Spectrum," arXiv preprint arXiv:1510.01392, 2015.

[28] Z. Tong and M. Haenggi, "Throughput analysis for full-duplex wireless networks with imperfect self-interference cancellation," IEEE Transactions on Communications, vol. 63, no. 11, pp. 4490–4500, 2015.

[29] Z. Yazdanshenasan, H. S. Dhillon, M. Afshang, and P. H. J. Chong, "Poisson hole process: Theory and applications to wireless networks," arXiv preprint arXiv:1601.01090, 2016.

[30] M. Haenggi, Stochastic Geometry for Wireless Networks. Cambridge University Press, 2012.

[31] J. Lee and T. Q. S. Quek, "Device-to-device communication in wireless mobile social networks," in 2014 IEEE 79th Vehicular Technology Conference (VTC Spring), pp. 1–5, May 2014.

[32] H. ElSawy, E. Hossain, and M.-S. Alouini, "Analytical modeling of mode selection and power control for underlay D2D communication in cellular networks," IEEE Transactions on Communications, vol. 62, no. 11, pp. 4147–4161, 2014.

[33] "Circle." http://www.ambrsoft.com/TrigoCalc/Sphere/Arc_$htm. Accessed$: $29 - 12 - 2018$.

NOMAN HAIDER Noman Haider received B.S. degree in electronics engineering from Mohammad Ali Jinnah University, Islamabad, Pakistan, in 2011 and his M.S. degree in electrical and electronics engineering from Universiti Teknologi Petronas, Malaysia, in 2014. He is currently a Ph.D. student in the School of Electrical and Data Engineering at the University of Technology Sydney, Australia. He has worked on different academic and industry sponsored projects in the field of wireless communications and networking. His research interests include modelling, analysis, and design of heterogeneous cellular networks in 5G.

AHSAN ALI Ahsan Ali received the B.S. (Hons) degree in electrical engineering from COMSATS Institute of Information Technology (CIIT), Pakistan in 2009, the M.Sc. degree in computer engineering from University of Engineering and Technology (UET), Taxila, Pakistan in 2011 and Master of Research (MRes) degree in 2015 from Macquarie University, Australia. Currently he is a PhD student in the department of Engineering, Macquarie University, Australia. During the period of 2009 to 2012 he worked at the Interactive Group of Companies (IAC), Pakistan, as an RF planning engineer. From 2012 to 2015 he was a Lecturer in the department of engineering, Hamdard University, Pakistan. For his academic excellence, Ahsan has received several academic awards including campus silver medal from CIIT, institute bronze medal from CIIT and several scholarships both local and international levels. Ahsan's research interest includes statistical modelling of asynchronous multi-carrier wireless networks and stochastic geometry analysis for wireless networks.

CRISTO SUAREZ-RODRIGUEZ Cristo Suarez-Rodriguez received the MSc degree in telecommunications engineering and the MRes degree in intelligent systems and numeric applications in engineering from the Universidad de Las Palmas de Gran Canaria, Las Palmas, Spain, in 2013 and 2015, respectively. He is currently pursuing the PhD degree at the Global Big Data Technologies Centre, University of Technology Sydney, Sydney, Australia. From 2010 to 2015, he was a Research Assistant with the Institute for Technological Development and Communication Innovation (IDeTIC), University of Las Palmas de Gran Canaria, Las Palmas, Spain. His research interest includes visible light communications and cellular communications with an emphasis on mobility management. Mr Suarez-Rodriguez was a recipient of the Accenture Award in New Services, Applications and Models of Digital Business in the 34th Spanish Official Association of Telecommunications Engineers Awards, Madrid, Spain, in 2014.

ERYK DUTKIEWICZ Eryk Dutkiewicz received the B.E. degree in electrical and electronic engineering and the M.Sc. degree in applied mathematics from The University of Adelaide in 1988 and 1992, respectively, and the Ph.D. degree in telecommunications from the University of Wollongong in 1996. His industry experience includes management of the Wireless Research Laboratory, Motorola, in early 2000's. He is currently the Head of the School of Electrical and Data Engineering, University of Technology Sydney, Australia. He is also a Professor with Hokkaido University, Japan. His current research interests cover 5G and IoT networks.